JOURNAL OF MATERIALS SCIENCE 26 (1991) 4220–4224

Microstructure change during crystallization of amorphous Bi(Pb)–Sr–Ca–Cu–O ceramics

S.-S. OH, K. OSAMURA
Department of Metallurgy, Kyoto University, Sakyo-ku, Kyoto 606, Japan

Amorphous Bi(Pb)–Sr–Ca–Cu–O ceramics can be obtained by quenching from the liquid. Microstructure change during crystallization has been investigated in detail. The $Bi_2Sr_2CuO_x$ (2201) phase crystallized first, followed by Cu_2O. This crystallization process began at a lower temperature in the specimen with Pb additive. The 2201 phase changed to the $Br_2Sr_2Ca_1Cu_2O_x$ (2212) phase during heating until partial melting began to occur. The 2212 phase changed to the $Bi_2Sr_2Ca_2Cu_3O_x$ (2223) phase under an existence of $(Sr, Ca)_3Cu_5O_x$ phase after a period of time.

1. Introduction

Since Maeda *et al.* [1] discovered a high T_c Bi–Sr–Ca–Cu–O superconducting ceramic, much effort has been made to elucidate the structure and phase relation of this complicated system. In the present Bi–Sr–Ca–Cu–O system, three kinds of perovskite superconducting phases have been reported to exist [2], as characterized by their chemical compositions $Bi_2Sr_2CuO_x$ (2201) superconducting phase, $Bi_2Sr_2CaCu_2O_x$ (2212) low T_c phase and $Bi_2Sr_2Ca_2Cu_3O_x$ (2223) high T_c phase. Komatsu *et al.* [3] demonstrated that a dense superconducting ceramic can be obtained by a melt-quenching method and the superconducting phase is crystallized from the amorphous state during annealing. Takano *et al.* [4] reported that the addition of Pb and prolonged heat treatment is most effective in increasing the volume fraction of (2223) high T_c phase. However, it was difficult [5] to produce the (2223) high T_c phase as a major phase using the melt-quenching and annealing technique. Another problem is that some impurity phases appear easily with the superconducting phases in the Bi–Sr–Ca–Cu–O system. It is important to clarify the phase relationship between the superconducting and impurity phases in order to produce only the (2223) high T_c single phase. However, few details have been reported up to now.

The present work aimed to clarify the relationship between the various phases which appeared during crystallization from the amorphous state obtained by melt-quenching. The influence of Pb addition on the crystallization process and the thermal stability of the superconducting phases has been investigated in detail.

2. Experimental procedure

Oxide powders of high-grade Bi_2O_3, $SrCO_3$, Ca_2CO_3, CuO and PbO were mixed and ground for 3.6 ks. The nominal compositions of the mixtures investigated were $Bi_2Sr_2Ca_2Cu_3O_x$ and $Bi_{1.6}Pb_{0.4}Sr_2Ca_2Cu_3O_x$. These two specimens are called here the specimen without and with Pb additive, respectively. The mixture was melted within a high-purity alumina crucible at 1443 K, at which the specimen was held only for a short time (0.6 ks) in order to avoid serious reaction of the melt with the crucible. The melt was poured on to a Cu plate and pressed by another Cu plate. A black glossy sheet ceramic, about 0.5 mm thick, was obtained by this procedure.

To examine the phase change during the crystallization process, the thermogravimetry and the differential thermal analysis (TG–DTA, Rigaku TAS 100 system) were performed in air at a heating rate of 0.083 K s^{-1}. In order to investigate the microstructure change, the specimen was heated at the same heating rate as for the TG–DTA measurements and then quenched into liquid N_2. This heat treatment (HT1) is shown schematically in Fig. 1. The isothermal heat-treatment (HT2) was performed at various temperatures for 86.4 ks in air and quenched into liquid N_2.

Identification of existing phases was made using an X-ray powder diffractometer (Philips PW1700 system, XRD) and electron probe microanalysis (EPMA). The microstructure was observed mainly by scanning electron microscopy (SEM).

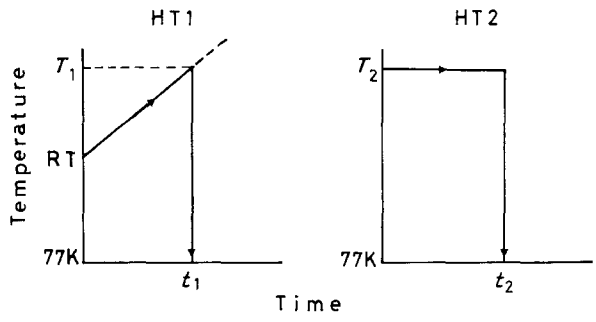

Figure 1 Schematic illustration of the two kinds of heat treatment employed here. HT1 indicates the continuous heating with constant rate and quenching, HT2 the isothermal annealing at a constant temperature and quenching.

0022–2461/91 $03.00 + .12

3. Results

Fig. 2 shows X-ray powder diffraction patterns for the specimen without additive as-quenched (a) and (b–d) after heat treatment HT1 up to various temperatures. The pattern (a) indicates an almost halo pattern characteristic of the amorphous phase and a small crystalline peak from CaO phase. Patterns (b), (c) and (d) indicate that various phases crystallized in sequence from the amorphous state during the heat treatment HT1.

Fig. 3 shows the results of TG–DTA measurements. As shown clearly in the DTA curves, a change appeared first at about 660–670 K, which has been reported by Komatsu *et al.* [3] to be caused by the glass transition. The transition temperature decreased on addition of Pb. Three exothermic peaks, marked A, B and C, appeared in common for specimens with and without Pb additive. The strongest endothermic peak, Y, which appeared at 1103 or 1113 K, was assigned to the onset temperature of partial melting. This temperature corresponds to the temperature at which the weight of the specimen began to decrease. To clarify the phase change during the crystallization process, the relative X-ray intensities were measured, where the diffraction peaks for each phase mentioned here are cited from other works [6–9].

Fig. 4 shows the change of X-ray intensity for the phases indicated in the figure as a function of temperature during heat treatment HT1. The relative intensity indicated here, is the ratio of the representative

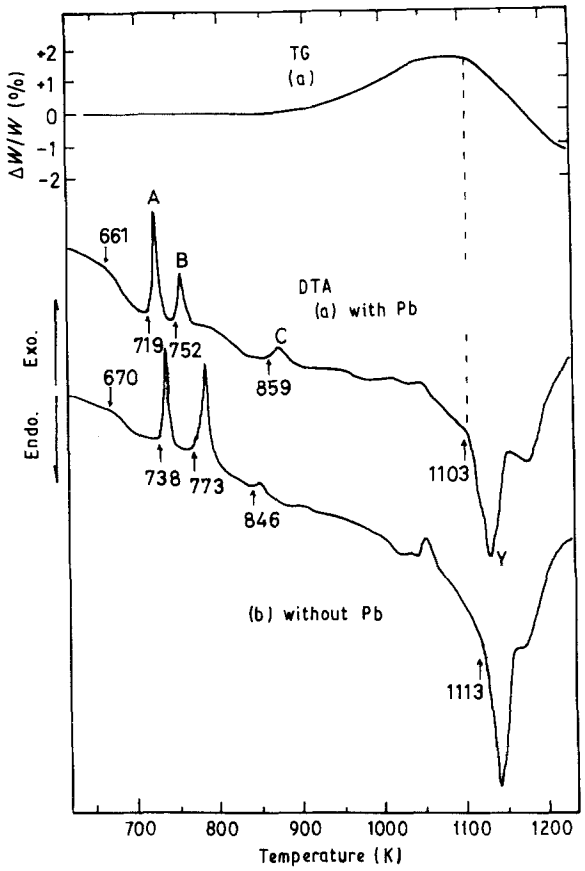

Figure 3 Results of TG and DTA measurement for the specimens (a) with and (b) without Pb additive.

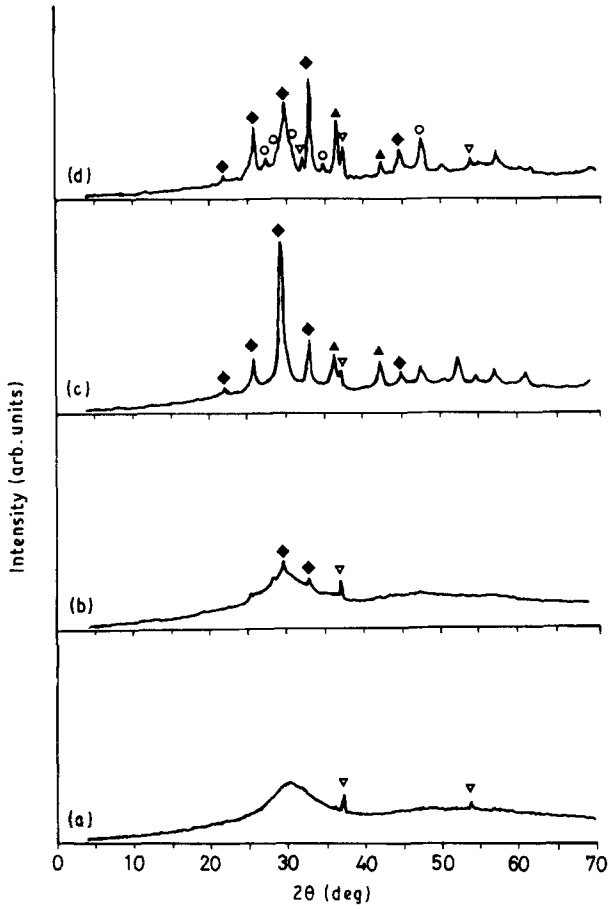

Figure 2 X-ray powder diffraction patterns for the specimens without additive heat treated by HT1. (a) As-quenched, (b) 773 K, (c) 823 K, (d) 923 K. (○) 2212, (▲) Cu_2O, (◆) 2201, (▽) CaO.

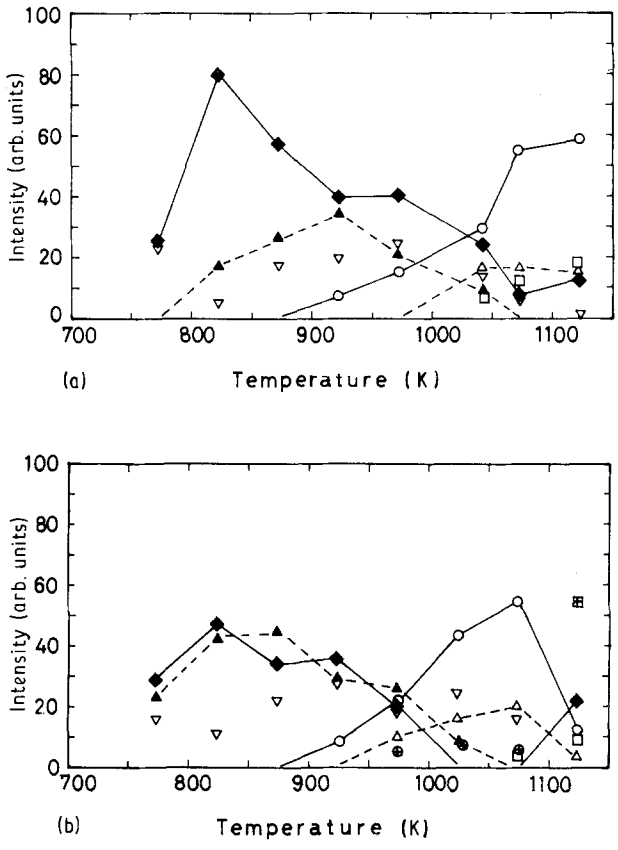

Figure 4 The change of relative X-ray intensity of the phases which appeared during heat treatment HT1 for the specimens (a) without and (b) with Pb additive. (◆) 2201, (▲) Cu_2O, (▽) CaO, (○) 2212, (△) CuO, (□) Ca_2CuO_3, (⊞) $(Sr, Ca)_3Cu_5O_x$, (⊕) Ca_2PbO_4.

peak intensity to the sum of all respective peak intensities, which can be used as a qualitative measure of the volume fraction of each phase. As shown in Fig. 4a, two crystalline phases, 2201 and CaO were observed to exist in the amorphous matrix at 773 K. Because CaO already exists in the as-quenched specimen, it is suggested that the first exothermic peak at 738 K, as shown in Fig. 3, corresponds to the crystallization of 2201 phase. This result is consistent with the reports of Ibara *et al.* [10] and Oka *et al.* [11]. As shown in Fig. 3, the crystallization of 2201 phase was found to occur at a lower temperature for the specimen with Pb additive. The second exothermic peak, B, which appeared at 773 K for the specimen without additive can be assigned to the crystallization of Cu_2O, because Cu_2O was first detected at temperatures lower than 823 K, as shown in Figs 2 and 4. The third exothermic peak, C, began to appear at 846 K for the specimen without additive. As shown in Fig. 2c and d, the 2212 phase appears at temperatures between 823 and 923 K. Therefore, the third exothermic peak, C, is suggested to correspond to the appearance of the 2212 phase. As shown in Fig. 4a, the relative X-ray intensity of the 2201 phase reached a maximum at 823 K and decreased gradually with increasing temperature, while the intensity of the 2212 phase was detected at 923 K and increased with increasing temperature up to 1123 K. From these results, it is suggested that the 2201 phase changes continuously into the 2212 phase. Two other phases, Cu_2O and CaO, should be related to this reaction. It was found that the Cu_2O phase starts to change into CuO at around 1000 K. Ca_2CuO_3 appeared at temperatures above 1020 K, where Ca was observed to be substituted for very small amount of Sr, by EPMA measurements.

As shown in Fig. 3, in the case of the specimen with Pb additive, the first and second exothermic peaks, A and B, appeared at lower temperatures. As shown in Fig. 4b, the 2201 phase disappeared at about 1023 K. However, the 2201 phase appeared again above 1100 K. The reason for this will be discussed later. The $(Sr, Ca)_3Cu_5O_x$ phase appeared at 1123 K. The Ca_2PbO_4 phase was observed in the temperature region between 973 and 1073 K.

Fig. 5 shows the change of relative X-ray intensity as a function of temperature for specimens after heat treatment HT2, where the specimen was isothermally annealed for 86.4 ks at various temperatures. In common for both specimens, as shown in Fig. 5a and b, is the relative intensity of the 2201 phase which decreased gradually with increasing temperature, while the 2212 phase appeared at 873 K. Cu_2O already existed at 773 K and changed into the CuO phase at lower temperatures. $(Sr, Ca)CuO_x$ appeared at 973 and 1073 K. It should be noted that the 2212, Ca_2CuO_3 and CuO for the specimen without additive exist at 1123 K, and the 2212, Ca_2CuO_3 and $(Sr, Ca)_3Cu_5O_x$ exist for the specimen with Pb additive. As the relative X-ray intensity of the 2212 phase is considerably higher than other phases, the 2212 phase is found to be a major phase at temperatures between 1073 and 1123 K.

Fig. 6 shows the change of the relative X-ray intensity as a function of annealing time at 1123 K for the specimen with Pb additive. The relative X-ray intensity of the 2212 phase increased gradually up to near 100 ks, while the 2201 phase decreased gradually and disappeared before 86.4 ks. It was considered that the growth of the 2212 phase occurred continuously with increasing annealing time. The 2201 phase was recognized to be unstable at 1123 K from the XRD results. On the other hand, the relative X-ray intensity of the Ca_2CuO_3 remained almost constant within the experimental conditions. Beyond 604.8 ks, the relative X-ray intensity of the 2212 phase decreased and the 2223 phase began to appear and its relative X-ray intensity increased with increasing annealing time.

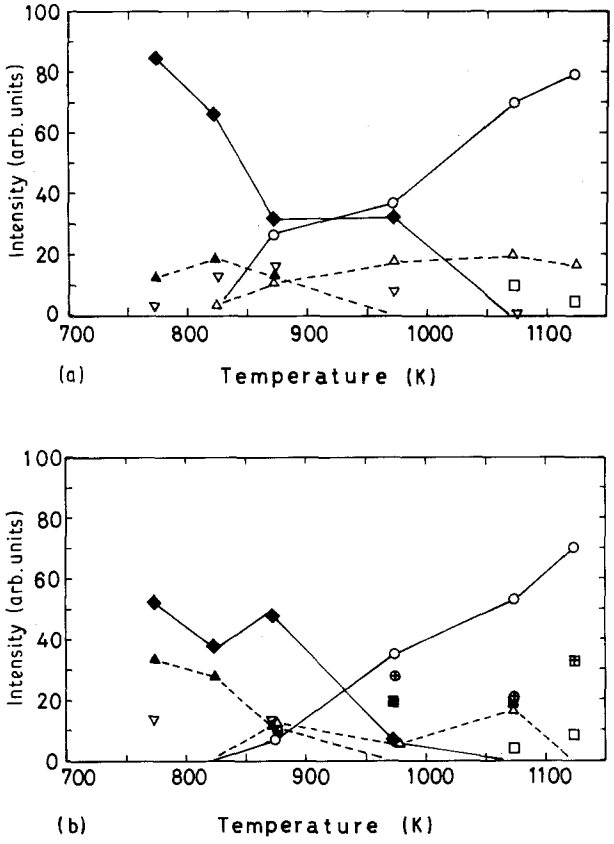

Figure 5 The change of relative X-ray intensity of the phases which appeared during heat treatment HT2 for the specimen (a) without and (b) with Pb additive. For key, see Fig. 4; (■) (Sr, Ca)CuO_x.

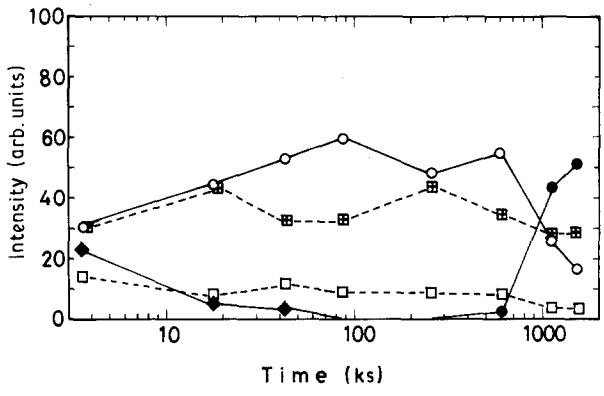

Figure 6 The change of relative X-ray intensity of the phases which appeared during isothermal annealing at 1123 K for the specimen with Pb additive. For key, see Fig. 4. (●) 2223.

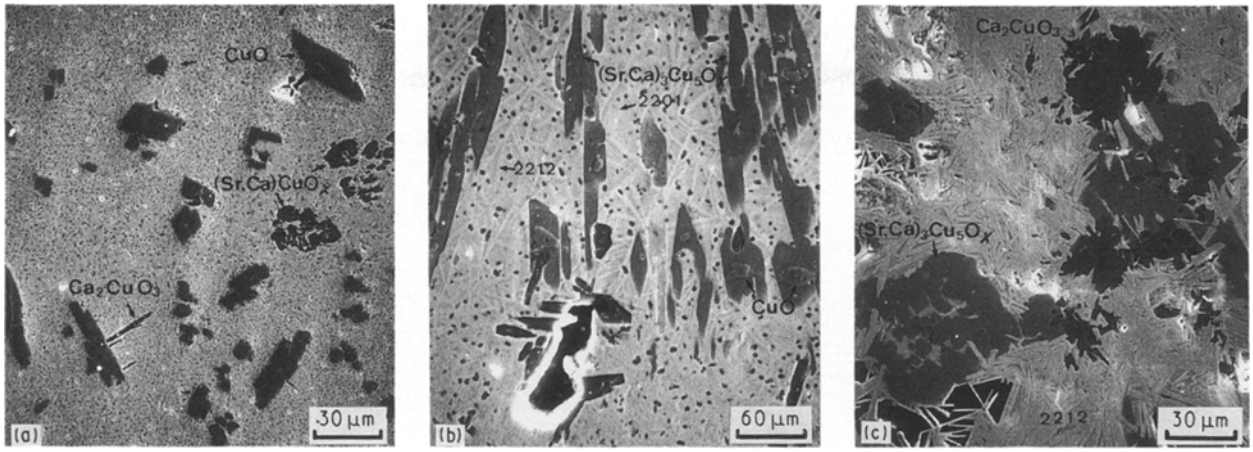

Figure 7 The microstructures for the specimen with Pb additive heat treated by HT1 ((a) 1073 K, (b) 1123 K) or (c) HT2 (1123 K, 86.4 ks).

4. Discussion

According to Noda *et al.* [12] and Oka *et al.* [13], the 2212 phase decomposes to CaO and a liquid at high temperatures above 1373 K. It seems to be reasonable to obtain the amorphous phase including the crystalline CaO phase by melt-quenching, when the specimen locates in the two-phase field of CaO solid phase, and the liquid at quenching temperature. As described above, it was determined that the 2201 phase crystallized first from the amorphous state. By this crystallization, the element Cu will be enriched around the crystalline phase and then the Cu-rich phase is crystallized. Crystallization of Cu_2O phase was confirmed to occur at temperatures between 752 and 773 K. As shown in Fig. 4a, the 2212 phase was detected at 923 K, which is crystallized from the remaining amorphous part by the mass balance of elements among the phases. This 2212 phase grows by absorbing the surrounding crystalline phases. During this process, the following reaction may occur

$$(2201) + CaO + \tfrac{1}{2}Cu_2O \rightarrow (2212) \quad (1)$$

Meanwhile, Oka *et al.* [11] reported that the structural change of the 2201 phase to 2212 phase occurs in the temperature range between 1023 and 1073 K for the $Bi_2Sr_2Ca_1Cu_2O_x$ specimens. As shown in Fig. 4, this change was found to occur at lower temperatures. This difference might result from their different nominal compositions.

Fig. 7a shows the microstructure at 1073 K for the specimen heat treated by HT1, where CuO, Ca_2CuO_3 and $(Sr, Ca)CuO_x$ were observed. The volume fraction of $(Sr, Ca)CuO_x$ phase was evaluated negligibly small. As shown in Fig. 7b, five phases, 2212, 2201, CuO, $(Sr, Ca)_3Cu_5O_x$ and Ca_2CuO_3 were detected at 1123 K for HT1 treatment. As CuO is observed inside the $(Sr, Ca)_3Cu_5O_x$ phase, a peritectic reaction is closely related to the formation of $(Sr, Ca)_3Cu_5O_x$ phase. The 2201 phase was observed with large volume fraction. Considering the above results, the following reaction can be suggested in the temperature range between 1073 and 1123 K.

$$(2212) + CuO \rightarrow \text{liquid} + (Sr, Ca)_3Cu_5O_x \quad (2)$$

accompanying a partial melting. During quenching, the liquid will be crystallized into 2201 phase. Fig. 7c shows the microstructure annealed at 1123 K for 86.4 ks. It was observed that four phases, 2212, 2201, Ca_2CuO_3 and $(Sr, Ca)_3Cu_5O_x$ coexist. The 2212 phase has grown with a plate-like shape and covered the matrix. As shown in Fig. 6, it was confirmed that the volume fraction of 2212 phase increased with increasing time up to 86.4 ks at 1123 K. The 2223 phase appeared at times longer than 604.8 ks, and was formed by the reaction of 2212 phase with $(Sr, Ca)_3Cu_5O_x$, because the X-ray intensities of the 2212 phase and $(Sr, Ca)_3Cu_5O_x$ decreased simultaneously, whereas the intensity for 2223 phase increased.

5. Conclusions

It could be confirmed that the 2201 phase and Cu_2O are crystallized in sequence from the amorphous phase during heating. These crystallizations occur at lower temperatures for the specimens with Pb additive. The 2201 phase changed to 2212 phase with increasing temperature up to a partial melting. It was also suggested that the 2212 phase reacts with CuO, and then the liquid appears, accompanied by $(Sr, Ca)_3Cu_5O_x$ phase. The 2223 phase is produced by prolonged heat treatment at 1123 K. It becomes clear that $(Sr, Ca)_3Cu_5O_x$ reacts with 2212 phase, and then the 2223 phase is formed.

Acknowledgements

We thank Messrs T. Unesaki and I. Nakagawa for their help in the EPMA and SEM analysis. This study was made possible by a Scientific Research Grant in-Aid (Project no. 01 644 520) from the Ministry of Education, Science and Culture of Japan.

References

1. H. MAEDA, Y. TAKADA, M. FUKUTOMI and T. ASANO, *Jpn J. Appl. Phys.* **27** (1988) L209.
2. H. MAEDA, in "Proceedings of Osaka University International Symposium on New Developments in Applied Superconductivity" edited by Y. Murakami (World Scientific, Singapore, 1989) p. 11.

3. T. KOMATSU, R. SATO, K. IMAI, K. MATSUSITA and T. YAMASHITA, *Jpn J. Appl. Phys.* **27** (1988) L550.
4. M. TAKANO, J. TAKADA, K. ODA, H. KITAGUCHI, Y. MIURA, Y. IKEDA, Y. TOMII and H. MAZAKI, *ibid.* **27** (1988) L550.
5. T. KOMATSU, R. SATO, C. HIROSE, K. MATSUSITA and T. YAMASHITA, *ibid.* **27** (1988) L2293.
6. H. MAZAKI, T. ISHIDA and T. SAKUMA, *ibid.* **27** (1988) L811.
7. S. KOYAMA, U. ENDO and T. KAWAI, *ibid.* **27** (1988) L1861.
8. K. ODA, H. KITAGUCHI, J. TAKADA, A. OSAKA, Y. MIURA, Y. IKEDA, M. TAKANO, Y. BANDO, Y. TOMII, Y. OKA, N. YAMAMOTO, Y. TAKEDA and H. MAZAKI, *J. Jpn Soc. Powder and Powder Metall.* **9** (1988) 153.
9. JCPDS card (JCPDS International Center for Diffraction Data, Park Lane, 1986).
10. Y. IBARA, H. NASU, T. IUMURA and Y. OSAKA, *Jpn J. Appl. Phys.* **28** (1989) L37.
11. Y. OKA, N. YAMAMOTO, H. KITAGUCHI, K. ODA and J. TAKADA, *Jpn J. Appl. Phys.* **28** (1989) L213.
12. T. NODA, T. IZUMI, A. NAKAMURA and Y. SHIOHARA, in "Advances in Superconductivity II", edited by T. Ishiguro and K. Kajimura (Springer-Verlag, Berlin, 1990) p. 239.
13. Y. OKA, N. YAMAMOTO, Y. TOMII, H. KITAGUCHI, K. ODA and J. TAKADA, *J. Jpn Soc. Powder and Powder Metall.* **36** (1989) 37.

Received 2 January
and accepted 19 November 1990